Retinoic acid-responsive CD8 effector T-cells are selectively increased in IL-23-rich tissue in gastrointestinal GvHD

Jennifer A. Ball[1], Andrew Clear[1], James Aries[1,3], Sarah Charrot[1,3], Caroline Besley[1], Matt Mee[1], Andrew Stagg[2], James O. Lindsay[2,4], Jamie Cavenagh[3], Maria Calaminci[1,5], John G. Gribben[1,3], Jeff Davies[1,3]

[1]Centre for Haemato-Oncology, Barts Cancer Institute, Queen Mary University of London, EC1M 6BQ, UK, [2] Centre for Immunobiology, Blizard Institute, Queen Mary University of London, and Departments of [3]Haemato-Oncology, [4]Gastroenterology, and [5]Histopathology, Barts Health NHS Trust, London UK

Corresponding author: Dr Jeff Davies

Address: Centre for Haemato-Oncology, Barts Cancer Institute, Queen Mary University of London, Charterhouse Square, London EC1M 6BQ

Phone: UK 0207 7882 3815

email: j.k.davies@qmul.ac.uk

Running Title: Retinoic acid-responsive T-cells in human GI-GvHD

Abstract word count: 250 Main text word count: 4350

Number of figures: 6 Number of tables: 2 Reference count: 45

Supplementary material (Supplementary Methods, Supplementary Tables 1-3, Supplementary Figures 1-14)

Visual Abstract

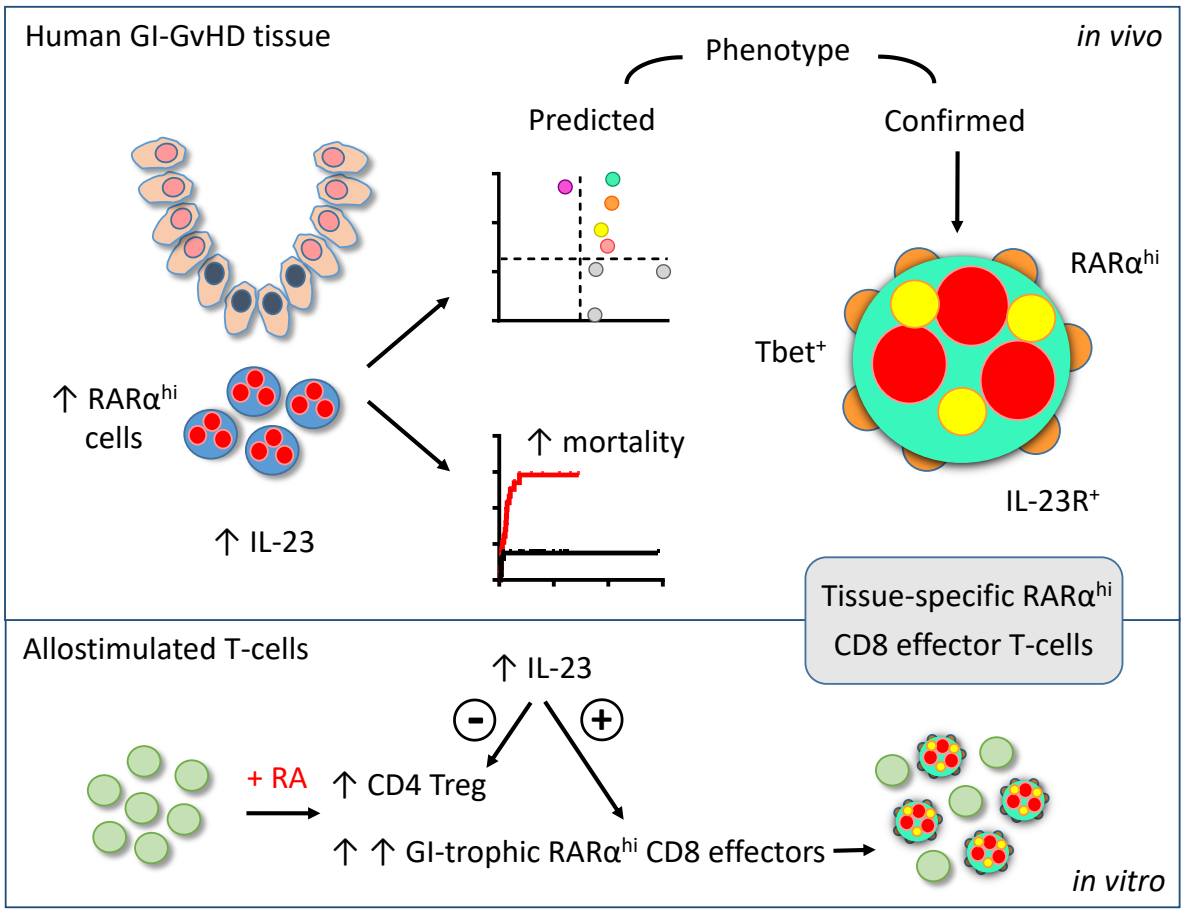

Key points

- RA-responsive mononuclear cells are increased in IL-23-rich human GI-GvHD tissue and are associated with poor outcome
- These cells have a GI-tropic IL-23R^{+} CD8 effector T-cell phenotype and are expanded by allostimulation in RA and IL-23-rich conditions

Abstract

Gastrointestinal (GI) graft-versus-host disease (GvHD) is a major barrier in allogeneic hematopoietic stem-cell transplantation (AHST). The metabolite retinoic acid (RA) potentiates GI-GvHD in mice via alloreactive T-cells expressing the RA-receptor-alpha (RARα), but the role of RA-responsive cells in human GI-GvHD remains undefined. We therefore used conventional and novel sequential immunostaining and flow cytometry to scrutinize RA-responsive T-cells in tissues and blood of AHST patients and characterize the impact of RA on human T-cell alloresponses. Expression of RARα by human mononuclear cells was increased after RA exposure. RARα^{hi} mononuclear cells were increased in GI-GvHD tissue, contained more cellular RA-binding proteins, localized with tissue damage and correlated with GvHD severity and mortality. Using a targeted candidate protein approach we predicted the phenotype of RA-responsive T-cells in the context of increased microenvironmental IL-23. Sequential immunostaining confirmed the presence of a population of RARα^{hi} CD8 T-cells with the predicted phenotype, co-expressing the effector T-cell transcription factor T-bet and the IL-23-specific receptor. These cells were increased in GI- but not skin-GvHD tissues and were also selectively expanded in GI-GvHD patient blood. Finally, functional approaches demonstrated RA predominantly increased alloreactive GI-tropic RARα^{hi} CD8 effector T-cells, including cells with the phenotype identified *in vivo*. IL-23-rich conditions potentiated this effect by selectively increasing β_7 integrin expression on CD8 effector T-cells and reducing CD4 T-cells with a regulatory cell phenotype. In conclusion we have identified a population of RA-responsive effector T-cells with a distinctive phenotype which are selectively expanded in human GI-GvHD and represent a potential new therapeutic target.

Introduction

Acute graft-versus-host disease (GvHD) is mediated by alloreactive donor T-cells that recognize and destroy healthy recipient tissues and results in significant morbidity and mortality after allogeneic hematopoietic stem-cell transplantation (AHST).[1-3] Acute GvHD can target the skin and liver, but patients with disease involving the gastrointestinal (GI) tract have the poorest outcome.[4] Current strategies to prevent GI-GvHD lack specificity and available therapies are unsatisfactory and cause significant toxicity. Better understanding of the tissue-specific pathways involved in the differentiation, expansion and migration of alloreactive donor T-cells which mediate GI-GvHD will permit better ways to prevent or treat this barrier to successful AHST.

Retinoic acid (RA), a metabolite of vitamin A, is a ligand for the nuclear RA receptors (RAR) α, β and γ which dimerize with retinoid X receptors at RA-response element sites to recruit co-activator proteins and promote gene transcription. The interaction of RA with RARα increases T-cell homing capacity to the GI-tract.[5] In addition, RA has diverse effects on immune cells by influencing both antigen-presenting cell (APC) function and T-cell differentiation. RA-signaling in the presence of TGF-β promotes immune tolerance *in vitro* by increasing CD4 regulatory T-cell numbers and reducing cytokine production by CD4 effector T-cells,[6,7] and RA production by APC in GI-associated lymphoid tissue contributes to maintenance of oral-antigen-induced tolerance *in vivo* in steady-state conditions.[8] However RA has also been shown to be essential for effector T-cell lineage stability,[9] and in pro-inflammatory conditions RA increases CD4 Th1 and Th17 effector T-cell responses[10] and potentiates CD8 effector T-cell differentiation.[11,12] Thus the immune effects of RA are context-dependent, contributing to maintenance of tolerance in steady-state conditions but promoting effector T-cell responses in inflammatory microenvironments.

Recent AHST studies in mice have shown that vitamin A-deficient diets reduce GI-GvHD,[13] and that RARα signaling in allogeneic donor T-cells potentiates GI-GvHD by increasing T-cell GI migration and also by modifying T-cell differentiation.[14,15] Furthermore, there is emerging

evidence that RA-dependent T-cell differentiation may be influenced by cytokines which are increased in GI-GVHD, including IL-23 which reduces RA-induced expansion of CD4 regulatory T-cells in other contexts,[16] and IL-33 which enhances RA-signaling in CD4 T-cells.[17] Thus RA and cytokines that influence the impact of RA on T-cell differentiation could represent important new therapeutic targets to prevent or treat GI-GvHD. However, the impact of RA at a tissue level in human GI-GvHD is currently unknown. We therefore combined analysis of tissue biopsies and peripheral blood from AHST patients and *in vitro* modelling to investigate the potential role of RA-responsive T-cells in human GI-GvHD.

Materials and Methods

Ethics approval

The study was approved by the London Research Ethical Committee (05/Q0605/140 and 06/Q0604/110) and conducted in accordance with the Declaration of Helsinki. Blood and tissue samples were obtained after signed informed consent from patients.

Patients and biopsies

Biopsies were performed for investigation of classical or late-onset acute GvHD in 54 AHST patients with hematologic malignancies or bone marrow failure (n=35 male, n=19 female, median age 51 years, range 20-66). Patients underwent granulocyte-colony-stimulating factor-mobilized peripheral blood stem-cell transplantation from HLA-matched (n=50, 93%) or single-antigen mismatched (n=4, 7%), related (n=20, 37%) or unrelated (n=34, 63%) donors using mostly fludarabine-based reduced-intensity conditioning (n=49, 91%), **Table 1**. All patients received uniform pharmacological immunoprophylaxis with short methotrexate and calcineurin inhibition weaned at D+90 in the absence of GvHD. 118 formalin-fixed paraffin-embedded biopsies (107 GI and 11 skin) from AHST patients performed prior to initiation of steroid therapy were studied and an additional 8 GI-biopsies from healthy controls with normal colonoscopies, **Supplementary Figures 1 and 2 and Supplementary Table 1**. Biopsies were independently reviewed by an expert histopathologist (MC) and histological GvHD confirmed using standard criteria.[18] Clinical organ-specific acute GvHD staging at time of biopsy used modified Glucksberg criteria.[19] Steroid-refractoriness was defined as no improvement after 14 days of 1-2mg/kg of prednisolone/equivalent. Peripheral blood CD3 T-cell donor chimerism was assessed at the time of first biopsy by variable number tandem repeat analysis as previously described, **Supplementary Figure 3.**

Conventional immunohistochemistry (IHC)

Appropriate negative and positive healthy tissue controls based on published expression patterns were used to optimize antibody staining, **Supplementary Figure 4**. Images were captured using an Olympus Ariol microscope and Ariol automated image analysis (Genetix, San Jose, CA) was used to identify and enumerate mononuclear cells based on hematoxylin nuclear counterstaining characteristics. Antibody staining was digitized, the mean intensity calculated from number of pixels/mononuclear cell. Cells were considered positive if intensity was equivalent to cells in positive controls and counted automatically using the Ariol system. RARα antibody staining (rabbit polyclonal, 1:4000, Santa Cruz, Dallas TX) and image analysis was titrated to identify only mononuclear cells with high RARα expression. We used two regional approaches to RARα^{hi} mononuclear cell enumeration; first we enumerated RARα^{hi} mononuclear cells in the whole biopsy, excluding epithelial areas which were diffusely positive for RARα making identification of the small numbers of intraepithelial RARα^{hi} mononuclear cells impossible. We also enumerated RARα^{hi} mononuclear cells in *sub-crypt regions* adjacent to basal crypts where GvHD-related epithelial stem-cell damage occurs, **Supplementary Figure 5**. Further technical details of antibody staining are detailed in **Supplementary Methods** and **Supplementary Table 2.**

Sequential immunostaining

Sequential immunostaining, stripping and re-probing on the same formalin-fixed paraffin-embedded biopsies was utilized to determine cellular co-expression of multiple markers.[20] After antigen retrieval, slides were stained with primary antibody, secondary antibody and VIP chromogen (as DAB could not be adequately stripped) and imaged before stripping by pressure-cooking and subsequent re-probing with the next antibody. Adequate stripping of primary antibodies was ensured by re-staining with secondary antibody and chromogen. Pannoramic Viewer v1.15.4 (3DHistech Ltd, Budapest, Hungary) was used to image cells.

Cells expressing high levels of staining were identified manually by the operator. To determine co-expression patterns of individual cells, each mononuclear cell within a minimum of 3 sub-crypt regions/biopsy was electronically marked and cellular expression of sequential immunostains was recorded, **Supplementary Figure 6**. The absolute number/unit area and proportion of mononuclear cells (minimum 200/biopsy) with each distinct expression pattern was collated. SPICE software version 5.3 (National Institute of Allergy and Infectious Disease) was used to depict frequencies of sub-populations of CD8 T-cells based on co-expression patterns of other molecules.

Patient blood samples, flow cytometry and cluster analysis

Flow cytometry used directly-conjugated antibodies, **Supplementary Table 3,** and viability dies to exclude dead cells. Analysis was performed using FlowJo software version 10 (LLC, Ashland, OR). tSNE plots were generated and cluster analysis was performed using Phenograph (https://bioconductor.org/packages/cytofkit/).[21]

Allogeneic co-cultures

Peripheral blood mononuclear cells (PBMC) were isolated by density gradient centrifugation from healthy blood donor filters or patient samples thirty days after AHST and labelled with a cell proliferation trackers CFSE (Invitrogen) or Cell Trace Violet (Invitrogen, Waltham MA). Labelled responders were co-cultured with equal numbers of irradiated HLA-mismatched allogeneic stimulator PBMC with *all-trans* RA (100mM-1μM*,* Sigma-Aldrich, St Louis MO), lipopolysaccharide (LPS, 1μg/ml, Sigma-Aldrich), human recombinant IL-23 (10ng/ml, Biolegend, San Diego CA) or vehicle controls in RPMI containing 10% FBS (Gibco, Gaithersburg, MD), 500iu penicillin and 0.5mg/ml streptomycin (Sigma-Aldrich). For some experiments the RARα-specific inhibitor ER-50891 (Santa Cruz) was added. Responder T-cell alloproliferation was determined on day 9 by cell label dilution as previously described.[22]

Statistical Methods

Two-tailed unpaired or paired tests were used to compare 2 groups as appropriate. Non-parametric tests were used for non-normally distributed datasets. Comparison of multiple groups used unpaired/paired ANOVA (equal groups) or mixed effects models (unequal groups) with post-test correction. Cumulative incidence of GI-GVHD-related mortality was calculated with non-GvHD-related mortality and disease relapse as competing risks. Statistical analysis was performed using Prism version 5.0 (Graphpad, San Diego CA) and STATA version 13 (Statacorp, College Station, TX).

Supplementary methods contain further detail of experimental and analytical techniques.

Data Sharing Statement: For original data please contact j.k.davies@qmul.ac.uk.

Results

RA-responsive mononuclear cells are increased in areas of GI-GvHD tissue damage

As cellular RA cannot be measured in fixed tissue, and prior studies have shown RA exposure increases RARα mRNA in antigen-stimulated T-cells,[24,25] we reasoned that cellular RARα expression could be used to identify RA-responsive cells. This was supported by initial observations that RARα protein expression was increased in PBMC by RA exposure during *in vitro* allostimulation, **Figure 1A-B.** We therefore developed an approach using conventional IHC to identify RA-responsive mononuclear cells with high RARα expression, **Figure 1C**, to scrutinize GI-biopsies from AHST patients with suspected GI-GvHD. Using this approach, RARα^{hi} cells represented a median of 17% (range 2-61%) of mononuclear cells in the entire non-epithelial area of GI-biopsies, and correlated with cells expressing cellular RA-binding proteins 1 and 2 (CRABPI/II) which reflect cellular RA content and deliver RA to nuclear RARs[26-28], **Figure 1D.** Regional analysis demonstrated significant enrichment of RARα^{hi} cells in sub-crypt regions adjacent to areas of epithelial stem cell damage in GI-GvHD, **Figure 1E-F**.

We next compared numbers of RARα^{hi} mononuclear cells in GI-biopsies with and without histological GvHD. Sub-crypt RARα^{hi} cell numbers were significantly higher in biopsies with histological GvHD than in biopsies from AHST patients without histological GvHD or from healthy controls, **Figure 1G-H.** Total CRABPI/II was also significantly increased in sub-crypt regions of GI-biopsies with histological GvHD, consistent with local enrichment of cellular RA, **Supplementary Figure 7**. Sub-crypt RARα^{hi} cell number had an optimal sensitivity and specificity of 77% and 91% respectively for presence of histological GvHD, with superior receiver-operator curve characteristics than RARα^{hi} staining intensity or number of CRABPI/II^{+} cells, **Figure 1I.** Importantly**,** sub-crypt RARα^{hi} mononuclear cells were significantly increased in biopsies with histological GvHD from both the upper and the lower GI tract **Figure 1J,** but

were not significantly different in biopsies grouped by patient, donor or other clinical factors including time to biopsy **Table 2.**

RARα^{hi} mononuclear cell numbers are associated with severity, response to treatment mortality of GI-GvHD

Sub-crypt RARα^{hi} cell numbers were significantly higher in patients with severe GI-GvHD (clinical stage 3-4) than in patients without GI-GvHD although RARα^{hi} cells numbers did not differentiate patients with non-severe (stage 1-2) GI-GvHD. However, when this analysis was restricted to lower GI-biopsies, RARα^{hi} cell numbers differentiated between patients with no GvHD, non-severe and severe GI-GvHD. Similarly, numbers of sub-crypt RARα^{hi} cells were significantly higher in lower GI biopsies from patients who were subsequently refractory to steroid therapy. Finally, we examined the association of sub-crypt RARα^{hi} cells with cumulative incidence (CI) of death attributable to GI-GvHD. We divided the patient cohort into tertiles according to sub-crypt RARα^{hi} mononuclear cell numbers. The CI of GI-GvHD-related death was significantly greater in patients with higher numbers of sub-crypt RARα^{hi} cells (76%, 32% and 10% in the first, second and third tertiles respectively, p= 0.002, Gray's Test). **Supplementary Figure 8.** Taken together these data support an important role for RA-responsive mononuclear cells in human GI-GvHD.

A targeted candidate protein approach identifies a predicted phenotype of RA-responsive cells in the context of increased microenvironmental IL-23

In view of these findings we next used conventional IHC to quantify T-cell lineage markers, transcription factors, and the cytokines IL-23 and IL-33 and their receptors in the same biopsy cohort to predict the likely phenotype of RA-responsive cells, **Figure 2A.** Including both upper and lower GI-biopsies, numbers of CD8 T-cells in sub-crypt regions were significantly

increased and CD4 T-cell numbers significantly decreased in biopsies with histological GvHD, **Figure 2B.**

Sub-crypt mononuclear cells expressing T-bet, a Th1/Tc1 effector T-cell transcription factor implicated in the pathogenesis of acute GvHD,[29] and cells expressing the regulatory T-cell transcription factor FOXP3 were significantly increased in biopsies with histological GvHD, whereas there was no significant change in cells expressing the Th17/Tc17 transcription factor ROR-γt.[30] In addition, cells expressing the IL-23p19 heterodimeric subunit of IL-23 (subsequently termed IL-23) and cells expressing the IL-23-receptor (R) were both significantly increased in biopsies with histological GvHD whereas cells expressing IL-33 and the IL-33R were not, **Figure 2C-D.** These findings persisted when analyses were restricted to either upper or lower GI-biopsies, **Supplementary Figure 9.** Importantly, in addition to an increase in number of IL-23^{+} cells, the total cellular IL-23 was also significantly increased in sub-crypt regions of GI biopsies with histological GvHD, **Figure 2E.** Finally, correlation analyses demonstrated that despite some intersample variation, RARα^{hi} cell numbers were modestly but significantly positively correlated with CD8 T-cells, cells expressing T-bet and cells expressing IL-23R, but not with numbers of cells expressing IL-23, **Figure 2F and Supplementary Figure 10.** These data are consistent with expansion of a population of RARα^{hi} CD8 T-cells co-expressing T-bet and IL-23R in GI-GvHD tissue in the context of increased microenvironmental IL-23.

Sequential immunostaining confirms the presence of tissue-specific RARα^{hi} CD8 effector T-cells co-expressing T-bet and IL-23R in GI-GvHD

To further delineate the phenotype of RA-responsive T-cells in GI-biopsies we utilized a novel approach using sequential immunostaining, stripping and re-probing to measure expression of multiple markers on single cells, **Figure 3A**. Importantly, we validated the accuracy of this approach by demonstrating close correlation between frequencies of cells enumerated with

the sequential immunostaining pipeline and manual counting approach with frequencies of cells enumerated with single-stain IHC and automated counting, **Figure 3B**.

We used sequential immunostaining to phenotype sub-crypt T-cells in 26 upper and lower GI-biopsies from 22 AHST patients and 4 healthy controls. Initial analyses confirmed a significant increase in RARα^{hi} CD8 T-cells in GI- biopsies with histological GvHD whereas there was no significant change in RARα^{hi} CD4 T-cells. In addition, numbers of CD8 T-cells, but not CD4 T-cells, expressing either T-bet or IL-23R were also significantly increased in biopsies with histological GvHD, **Figures 4A-D**. and **Supplementary Figure 11 A-B**. In view of this we next enumerated 8 phenotypically distinct subpopulations of CD8 T-cells based on co-expression patterns of RARα, T-bet and IL-23R. Importantly, the only CD8 T-cell sub-population present in significantly increased proportions in GI-biopsies with histological GvHD co-expressed high levels of RARα, T-bet and IL-23R (*triple positive* cells) **Figure 4E-F**. This translated into a significant increase in the absolute number of triple positive CD8 T-cells in GI-biopsies with histological GvHD, **Figure 4G**, which was also seen when analysis was restricted to lower GI-biopsies, **Supplementary Figure 11C-D.**

In order to asses if this novel population of triple positive CD8 effector T-cells was specific to GI tissues, we also performed sequential immunostaining staining on skin biopsies from 11 AHST patients. There was no increase in the proportion of triple positive CD8 T-cells in skin biopsies with histological GvHD, **Figure 4H**. These findings support GI-tissue specificity of the triple positive CD8 T-cell effector population.

Finally, as RA expands CD4 regulatory T-cells under some conditions,[6,7] and we had found increased FOXP3^{+} mononuclear cells in GI-biopsies with histological GvHD, we also enumerated FOXP3^{+} CD4 T-cells using sequential immunostaining. Despite a reduction in overall RARα^{hi} CD4 T-cells, RARα^{hi} FOXP3^{+} CD4 T-cells were modestly increased in GI-biopsies with histological GvHD, although these biopsies had 5-fold more RARα^{hi} CD8 effector T-cells than RARα^{hi} FOXP3^{+} CD4 T-cells, consistent with a net pro-inflammatory effect of RA-responsive T-cells, **Figure 4I**.

RARα^{hi} effector T-cells are also selectively expanded in the peripheral blood of GI-GvHD patients

We next quantified RARα^{hi} T-cell populations in peripheral blood of patients after AHST. Frequencies of triple positive CD8 T-cells were significantly increased in peripheral blood of GI-GvHD patients compared to skin GvHD patients, patients without GvHD or healthy controls **Figure 5A-B**. In contrast, there was no significant increase in the frequency of RARα^{hi} or triple positive CD4 T-cells in peripheral blood of GI-GvHD patients, **Figure 5C**.

In order to assess GI-tissue selectivity of peripheral blood RARα^{hi} CD8 effector T-cells, we also measured co-expression of molecules which confer GI-migratory capacity including the β_7 subunit of the $\alpha_4\beta_7$ integrin (as α_4 is expressed on more than 90% of peripheral blood T-cells) and CCR9. To contextualize these cells within broader immune reconstitution we performed unsupervised phenotypic clustering analysis on all live mononuclear cells. Using expression of 7 cell surface and intracellular molecules we identified 24 phenotypically distinct T-cell clusters, 12 of which were T-cell populations, **Figure 5D-E**. Only one (cluster 4) was present at significantly increased abundance in peripheral blood from GI- but not skin GvHD patients or healthy controls, which possessed the triple positive phenotype, expressed both β_7 and CCR9, and was expanded to a median frequency of 10% of live mononuclear cells in GI-GvHD patients, **Figure 5F-H.**

The dominant effect of RA on human alloresponses is an increase in GI-tropic RARα^{hi} CD8 effector T-cells

In view of the selective expansion of RARα^{hi} CD8 effector T-cells we had demonstrated in both GI tissue and blood of GI-GvHD patients, we used allogeneic healthy donor PBMC co-cultures to investigate the impact of exogenous (*all trans*) RA on human T-cell alloresponses.

At lower doses of RA alloproliferation of both CD8 and CD4 T-cells was preserved. However, at higher doses of RA alloproliferation of CD8 T-cells was not significantly impacted whereas CD4 T-cell alloproliferation was significantly reduced (median 30% reduction), **Figure 6A**.

Predictably, RA increased expression of GI-tropic molecules on both alloproliferative CD8 and CD4 T-cells, with maximum upregulation at 1µm concentrations, **Supplementary Figure 12**. Notably RA at 1µM concentrations also significantly increased the proportion of alloproliferative CD8 T-cells expressing high levels of RARα, the activation marker CD25, and the effector cell transcription factor T-bet, **Figure 6B**. A similar increase in the proportion of activated alloproliferative CD8 T-cells expressing CD25 was seen with RA added at the beginning of co-culture or at later time points, consistent with a direct effect on alloreactive T-cells rather than an effect on APC, and CD8 effector T-cells expressing T-bet were found predominantly within the $RAR\alpha^{hi}$ CD8 T-cell compartment after RA exposure, as were cells upregulating GI-tropic molecules, **Supplementary Figure 13A-C.** Exogenous RA resulted in a 2-fold increase in alloproliferative CD8 T-cells with the triple positive phenotype we had identified in tissue and blood of patients with GI-GvHD and a 5-fold increase in triple positive CD8 T-cells expressing GI-homing molecules, which was effectively blocked by a specific inhibitor of the RARα receptor, **Figure 6B**, as was expansion of CD8 T-cells expressing each individual protein, **Supplementary Figure 13D**, demonstrating that the effect is mediated by RARα ligation..

In contrast RA exposure did not increase the proportion of alloproliferative CD4 effector T-cells expressing high levels of T-bet, but did increase the proportion co-expressing CD25 and FOXP3 reflecting an increase in cells with a $CD25^{hi}FOXP3^{+}$ regulatory T-cell phenotype, **Supplementary Figure 13E.** However, RA exposure resulted in significantly larger increases in alloproliferative CD8 effector T-cells than in CD4 $FOXP3^{+}$ cells**,** consistent with a net pro-inflammatory effect on T-cell alloresponses and mirroring our findings in GI-GvHD tissue biopsies.

Importantly, RA exposure induced similar phenotypic changes in alloproliferative T-cells in peripheral blood samples from AHST patients, **Supplementary Figure 13 F-G**.

IL-23-rich conditions potentiate selective expansion of RA-responsive GI-tropic alloreactive CD8 effector T-cells

As we had found IL-23^{+} mononuclear cells and RARα^{hi} CD8 effector T-cells expressing the IL-23R were both increased in GI-GvHD tissues we next sought to determine the impact of the combination of IL-23 and RA on human T-cell alloresponses. Increased frequencies of RARα^{hi} CD8 effector T-cells were maintained with IL-23 and RA during allostimulation, but not significantly higher than with RA alone, **Figure 6D and Supplementary Figure 14A-D**. In contrast, the combination of RA and IL-23 resulted in significantly more alloproliferative CD8 T-cells expressing the β_7 integrin subunit and co-expressing both the α_4 and β_7 integrin subunits than RA or IL-23 alone, an effect that was not seen in alloproliferative CD4 T-cells, **Figure 6 D-E** and **Supplementary Figure 14E-G**. The increased expression of β_7 induced by IL-23 and RA was largely restricted to RARα^{hi} CD8 T-cells, resulting in a significant increase in β_7 expression on CD8 effector T-cells with the triple positive phenotype identified *in vivo,* **Supplementary Figure 14H.** Importantly, IL-23 also significantly reduced RA-induced expansion of FOXP3^{+} CD4 T-cells, **Supplementary Figure 14I**, increasing the ratio of CD8 effectors to FOXP3^{+} CD4 T-cells within the alloproliferative compartment, **Figure 6F.**

Finally, in order to assess the impact of wider IL-23-rich pro-inflammatory environments on RA-responsive T-cell alloresponses we examined the effect of lipopolysaccharide (LPS), which is increased in GI tissue after AHST, induces macrophages to release IL-23 and provides multiple additional pro-inflammatory signals.[31] LPS alone did not significantly increase alloproliferative RA-responsive CD8 effector T-cells whereas RA and LPS significantly increased frequencies of alloproliferative CD8 effector T-cells including cells with a GI-tropic triple positive phenotype, **Figure 6G.** This larger expansion facilitated phenotypic cluster analysis we had used in patient blood samples, **Figure 6H-I.** A single cluster of

alloproliferative CD8 effector T-cells was present at significantly higher frequency after RA and LPS exposure with a triple positive GI-tropic phenotype similar to that identified in peripheral blood of GI-GvHD patients**.** Notably this cluster had bright expression of β_7 consistent with the effect we had identified *in vitro* with IL-23 and RA, **Figure 6J-L.**

Taken together these data are consistent with IL-23 increasing GI-recruitment and/or retention of RA-responsive alloreactive CD8 effector T-cells and also limiting RA-induced expansion of CD4 T-cells with a regulatory phenotype, resulting in a net pro-inflammatory effect.

Discussion

In this study we show that RA-responsive T-cells are selectively increased at sites of GI-GvHD tissue damage in humans in the context of increased IL-23, and correlate with disease severity and mortality. Furthermore, we characterized these cells as predominantly CD8 effector T-cells expressing high levels of RARα, T-bet and IL-23R. Our functional experiments confirm the dominant effect of RA on human T-cell alloresponses is to increase GI-tropic CD8 effector T-cells and is potentiated in IL-23-rich environments. Selectively targeting of this RA-responsive CD8 effector T-cell population could provide a new strategy to prevent or treat GI-GvHD.

We studied patient biopsies from both the upper and lower GI-tract although most patients had biopsies from either just the lower GI-tract or from both sites. Although studies have shown that lower GI-GvHD has a more significant impact than upper GI-GVHD on GvHD-related mortality,[32] upper GI pathology may increase lower GI-GvHD symptoms.[33] Importantly, although numbers of RA-responsive cells in lower GI-biopsies were more closely associated with clinical severity of GI-GvHD than numbers in upper GI-biopsies, we found an increase in RA-responsive cells in both upper and lower GI-biopsies supporting a pathogenic role for RA-responsive cells throughout the GI-tract.

Intriguingly, several GI-biopsies without histological GvHD had evidence of alternative infective/inflammatory processes despite low levels of RA-responsive cells. However, the role of RA-responsive cells in AHST patients with CMV colitis, which can occur after post-transplant and were not included in our study, will be important to further assess the specificity of these cells.

To our knowledge no prior studies have examined the role of RA at a tissue level in human GI-GvHD, although multiple animal studies have shown vitamin A depletion, which reduces tissue RA levels, selectively reduces GI-GvHD.[34,35] Intriguingly, a recent study in pediatric transplant recipients found GI-GvHD was associated with low plasma vitamin A levels. [36]

Although we did not measure the plasma Vitamin A levels in our patients, but we show RA-responsive effector T-cells and levels of RA-binding proteins (which are proportional to cellular RA content) were increased in GI-GvHD tissues. The precise relationship between plasma vitamin A levels and cellular RA levels in GI tissue remains to be determined, but our current findings highlight the importance of scrutinizing the GI-microenvironment where metabolite concentrations may be regionally concentrated.

Our findings are consistent with recent murine studies that show GI-GvHD is mediated by RA-responsive T-cells with increased RARα expression.[14,15] In contrast to the findings in mice, despite RA upregulating GI-tropic molecules on alloproliferative CD8 and CD4 cells, we found only increases in RARα^{hi} CD8 effector cells in GI-GvHD biopsies. One explanation for this may have been the selective reduction in CD4 alloproliferation we observed after *in vitro* RA exposure, potentially reflecting differential RA-response element utilization in murine and human T-cells. However, in common with these murine studies we found larger increases in RA-responsive effector T-cells were accompanied by smaller increases in CD4 T-cells with a regulatory phenotype in GI-GvHD tissue and after *in vitro* allostimulation in the presence of RA. This qualitatively distinct action of RA on human CD8 and CD4 T-cell alloresponses could represent a therapeutic opportunity if the two effects could be dissociated or selectively manipulated.

Although most prior studies report T-cell infiltrates in human GI-GvHD tissue are predominantly CD8 T-cells,[37,38] other studies show pathogenic CD4 T-cells play a role which may be licensed by microenvironmental factors other than RA.[39-41] It is therefore likely that RA-responsive CD8 effector T-cells represent one of several distinct immune cell subsets contributing to the pathogenesis of GI-GvHD and the temporal distinction, interplay and functional dominance between RA-responsive CD8 effector T-cells and these other cell subsets remains to be determined.

Although we did not directly demonstrate a causal role for IL-23 in selectively concentrating RA-responsive CD8 effector T-cells *in vivo* our findings suggest that IL-23, which modulates

T-cell responses to RA in other contexts may be one of the local factors influencing RA-responsive T-cell alloresponses in the GI-microenvironment. Mononuclear cells expressing IL-23 were increased in GI-GvHD tissues but did not correlate with RARα^{hi} or CD8 T-cells, consistent with a *trans* effect on RA-responsive CD8 T-cells. IL-23 has been implicated in the pathogenesis of both murine and human GI-GvHD,[42,43] and IL-23p19-specific blockade is in clinical use for autoimmune disease. However, as only half of RARα^{hi} CD8 effector T-cells-in GI-GvHD tissues expressed the IL-23R, our results support targeting IL-23 as an adjunct but not an alternative to directly targeting RA-responsive CD8 effector T-cells. Furthermore, we cannot exclude the contribution of untested microenvironmental factors in licensing RA-responsive CD8 effector T-cells, and the larger effect seen *in vitro* with LPS and RA compared to IL-23 and RA suggest that additional LPS-induced signals are also likely to contribute to the expansion of these pathogenic cells.

The vast majority of biopsies in our study were from patients who had undergone AHST using reduced-intensity conditioning. Although this approach is commonly applied worldwide, we do not yet know if our findings can be generalized more widely to other full-intensity conditioning transplant platforms. Although it will be important to validate our findings after more intensive AHST conditioning including those containing total body irradiation, it is likely that expansion of RA-responsive effector T-cells also occurs in GI-GvHD in this setting as total body irradiation increases both LPS release and RA-signaling in the GI microenvironment in mice.[44,45]

Further exploration of mechanisms by which RA directs alloreactive T-cell differentiation will be key for translation of our findings into strategies to prevent or treat GI-GvHD. Although RARα blockade is in development in other clinical contexts, this direct approach may not be optimal in the context of GI-GvHD as RA also has an important role in maintaining GI-mucosal integrity and Vitamin A deprivation in transplanted mice can redirect GvHD to other target organs.[34,35]. Identification of the individual RA-response elements in human alloreactive CD8

and CD4 T-cells could facilitate targeted therapeutic intervention, potentially uncoupling the impact of RA on CD8 effector T-cells and regulatory CD4 T-cells to promote tolerogenic T-cell alloresponses within GI tissue.

Acknowledgements

This work was supported by grants from by Bloodwise (Project Grant 15007) and CRUK (Barts Cancer Centre grant)

Authorship

Contribution: JB performed and analyzed IHC/sequential immunostaining of biopsies, designed, performed and analyzed patient peripheral blood and allogeneic co-culture experiments, and wrote the manuscript. AC optimized and performed IHC and sequential immunostaining of tissue biopsies. JA performed tSNE/cluster analysis of patient peripheral blood and in vitro data. SC, CB and MM contributed to experimental design and data analysis and contributed to the writing of the manuscript. AS and JL contributed to the conception of the project and experimental design. JDC contributed patient samples. MC contributed to the conception of the project and performed histological review of tissue biopsies. JGG contributed to the conception of the project, contributed patient samples, contributed to experimental design and the writing of the manuscript. JKD conceived, designed and supervised the study, analyzed and interpreted experiments and clinical data and wrote the manuscript. All authors approved the final manuscript.

COI disclosures: None declared

Correspondence: Dr Jeff Davies, Centre for Haemato-Oncology, Barts Cancer Institute, Queen Mary University of London, Charterhouse Square, London EC1M 6BQ Phone: UK 0207 7882 3815 email: j.k.davies@qmul.ac.uk

References

1. Anasetti C, Logan BR, Lee SJ, et al. Peripheral-blood stem cells versus bone marrow from unrelated donors. *N Engl J Med*. 2012;367(16):1487-1496.

2. Saber W, Opie S, Rizzo JD, Zhang MJ, Horowitz MM, Schriber J. Outcomes after matched unrelated donor versus identical sibling hematopoietic cell transplantation in adults with acute myelogenous leukemia. *Blood*. 2012;119(17):3908-3916.

3. Wagner JE, Thompson JS, Carter SL, Kernan NA, Unrelated Donor Marrow Transplantation T. Effect of graft-versus-host disease prophylaxis on 3-year disease-free survival in recipients of unrelated donor bone marrow (T-cell Depletion Trial): a multi-centre, randomised phase II-III trial. *Lancet*. 2005;366(9487):733-741.

4. Castilla-Llorente C, Martin PJ, McDonald GB, et al. Prognostic factors and outcomes of severe gastrointestinal GVHD after allogeneic hematopoietic cell transplantation. *Bone Marrow Transplant*. 2014;49(7):966-971.

5. Iwata M, Hirakiyama A, Eshima Y, Kagechika H, Kato C, Song SY. Retinoic acid imprints gut-homing specificity on T-cells. *Immunity*. 2004;21(4):527-538.

6. Coombes JL, Siddiqui KR, Arancibia-Carcamo CV, et al. A functionally specialized population of mucosal CD103+ DCs induces Foxp3+ regulatory T-cells via a TGF-beta and retinoic acid-dependent mechanism. *J Exp Med*. 2007;204(8):1757-1764.

7. Mucida D, Park Y, Kim G, et al. Reciprocal TH17 and regulatory T-cell differentiation mediated by retinoic acid. *Science*. 2007;317(5835):256-260.

8. Sun CM, Hall JA, Blank RB, et al. Small intestine lamina propria dendritic cells promote de novo generation of Foxp3 T reg cells via retinoic acid. *J Exp Med*. 2007;204(8):1775-1785.

9. Brown CC, Esterhazy D, Sarde A, et al. Retinoic acid is essential for Th1 cell lineage stability and prevents transition to a Th17 cell program. *Immunity*. 2015;42(3):499-511.

10. Hall JA, Cannons JL, Grainger JR, et al. Essential role for retinoic acid in the promotion of CD4(+) T-cell effector responses via retinoic acid receptor alpha. *Immunity*. 2011;34(3):435-447.

11. Allie SR, Zhang W, Tsai CY, Noelle RJ, Usherwood EJ. Critical role for all-trans retinoic acid for optimal effector and effector memory CD8 T-cell differentiation. *J Immunol*. 2013;190(5):2178-2187.

12. Tan X, Sande JL, Pufnock JS, Blattman JN, Greenberg PD. Retinoic acid as a vaccine adjuvant enhances CD8+ T-cell response and mucosal protection from viral challenge. *J Virol*. 2011;85(16):8316-8327.

13. Dodge J, Stephans A, Lai J, Drobyski WR, Chen X. Effects of Donor Vitamin A Deficiency and Pharmacologic Modulation of Donor T-cell Retinoic Acid Pathway on the Severity of Experimental Graft-versus-Host Disease. *Biol Blood Marrow Transplant*. 2016;22(12):2141-2148.

14. Chen X, Dodge J, Komorowski R, Drobyski WR. A critical role for the retinoic acid signaling pathway in the pathophysiology of gastrointestinal graft-versus-host disease. *Blood*. 2013;121(19):3970-3980.

15. Aoyama K, Saha A, Tolar J, et al. Inhibiting retinoic acid signaling ameliorates graft-versus-host disease by modifying T-cell differentiation and intestinal migration. *Blood*. 2013;122(12):2125-2134.

16. DePaolo RW, Abadie V, Tang F, et al. Co-adjuvant effects of retinoic acid and IL-15 induce inflammatory immunity to dietary antigens. *Nature*. 2011;471(7337):220-224.

17. Gajardo T, Perez F, Terraza C, Campos-Mora M, Noelle RJ, Pino-Lagos K. IL-33 enhances retinoic acid signaling on CD4+ T-cells. *Cytokine*. 2016;85:120-122.

18. Kreft A, Mottok A, Mesteri I, et al. Consensus diagnostic histopathological criteria for acute gastrointestinal graft versus host disease improve interobserver reproducibility. *Virchows Arch*. 2015;467(3):255-263.

19. Przepiorka D, Weisdorf D, Martin P, et al. 1994 Consensus Conference on Acute GVHD Grading. *Bone Marrow Transplant*. 1995;15(6):825-828.

20. van den Brand M, Hoevenaars BM, Sigmans JH, et al. Sequential immunohistochemistry: a promising new tool for the pathology laboratory. *Histopathology*. 2014;65(5):651-657.

21. Levine JH, Simonds EF, Bendall SC, et al. Data-Driven Phenotypic Dissection of AML Reveals Progenitor-like Cells that Correlate with Prognosis. *Cell*. 2015;162(1):184-197.

22. Kotsiou E, Okosun J, Besley C, et al. TNFRSF14 aberrations in follicular lymphoma increase clinically significant allogeneic T-cell responses. *Blood*. 2016;128(1):72-81.

23. Camp RL, Dolled-Filhart M, Rimm DL. X-tile: a new bio-informatics tool for biomarker assessment and outcome-based cut-point optimization. *Clin Cancer Res*. 2004;10(21):7252-7259.

24. Friedman A, Halevy O, Schrift M, Arazi Y, Sklan D. Retinoic acid promotes proliferation and induces expression of retinoic acid receptor-alpha gene in murine T lymphocytes. *Cell Immunol*. 1993;152(1):240-248.

25. Halevy O, Arazi Y, Melamed D, Friedman A, Sklan D. Retinoic acid receptor-alpha gene expression is modulated by dietary vitamin A and by retinoic acid in chicken T lymphocytes. *J Nutr*. 1994;124(11):2139-2146.

26. Donato LJ, Noy N. Fluorescence-based technique for analyzing retinoic acid. *Methods Mol Biol*. 2010;652:177-187.

27. Dong D, Ruuska SE, Levinthal DJ, Noy N. Distinct roles for cellular retinoic acid-binding proteins I and II in regulating signaling by retinoic acid. *J Biol Chem*. 1999;274(34):23695-23698.

28. Budhu AS, Noy N. Direct channeling of retinoic acid between cellular retinoic acid-binding protein II and retinoic acid receptor sensitizes mammary carcinoma cells to retinoic acid-induced growth arrest. *Mol Cell Biol*. 2002;22(8):2632-2641.

29. Fu J, Wang D, Yu Y, et al. T-bet is critical for the development of acute graft-versus-host disease through controlling T-cell differentiation and function. *J Immunol*. 2015;194(1):388-397.

30. Haines CJ, Chen Y, Blumenschein WM, et al. Autoimmune memory T helper 17 cell function and expansion are dependent on interleukin-23. *Cell Rep*. 2013;3(5):1378-1388.

31. Arango Duque G, Descoteaux A. Macrophage cytokines: involvement in immunity and infectious diseases. *Front Immunol*. 2014;5:491.

32. Nikiforow S, Wang T, Hemmer M, et al. Upper gastrointestinal acute graft-versus-host disease adds minimal prognostic value in isolation or with other graft-versus-host disease symptoms as currently diagnosed and treated. *Haematologica*. 2018;103(10):1708-1719.

33. Joshi NM, Hassan S, Jasani P, et al. Bile acid malabsorption in patients with graft-versus-host disease of the gastrointestinal tract. *Br J Haematol*. 2012;157(3):403-407.

34. Koenecke C, Prinz I, Bubke A, et al. Shift of graft-versus-host-disease target organ tropism by dietary vitamin A. *PLoS One*. 2012;7(5):e38252.

35. Martin JC, Beriou G, Heslan M, et al. IL-22BP is produced by eosinophils in human gut and blocks IL-22 protective actions during colitis. *Mucosal Immunol*. 2016;9(2):539-549.

36. Lounder DT, Khandelwal P, Dandoy CE, et al. Lower levels of vitamin A are associated with increased gastrointestinal graft-versus-host disease in children. *Blood*. 2017;129(20):2801-2807.

37. Rieger K, Loddenkemper C, Maul J, et al. Mucosal FOXP3+ regulatory T-cells are numerically deficient in acute and chronic GvHD. *Blood*. 2006;107(4):1717-1723.

38. Roy J, Platt JL, Weisdorf DJ. The immunopathology of upper gastrointestinal acute graft-versus-host disease. Lymphoid cells and endothelial adhesion molecules. *Transplantation*. 1993;55(3):572-578.

39. Betts BC, Sagatys EM, Veerapathran A, et al. CD4+ T-cell STAT3 phosphorylation precedes acute GVHD, and subsequent Th17 tissue invasion correlates with GVHD severity and therapeutic response. *J Leukoc Biol*. 2015;97(4):807-819.

40. Furlan SN, Watkins B, Tkachev V, et al. Systems analysis uncovers inflammatory Th/Tc17-driven modules during acute GVHD in monkey and human T-cells. *Blood*. 2016;128(21):2568-2579.

41. Zhou V, Agle K, Chen X, et al. A colitogenic memory CD4+ T-cell population mediates gastrointestinal graft-versus-host disease. *J Clin Invest*. 2016;126(9):3541-3555.

42. Das R, Chen X, Komorowski R, Hessner MJ, Drobyski WR. Interleukin-23 secretion by donor antigen-presenting cells is critical for organ-specific pathology in graft-versus-host disease. *Blood*. 2009;113(10):2352-2362.

43. Shono Y, Docampo MD, Peled JU, et al. Increased GVHD-related mortality with broad-spectrum antibiotic use after allogeneic hematopoietic stem cell transplantation in human patients and mice. *Sci Transl Med*. 2016;8(339):339ra371.

44. Hill GR, Crawford JM, Cooke KR, Brinson YS, Pan L, Ferrara JL. Total body irradiation and acute graft-versus-host disease: the role of gastrointestinal damage and inflammatory cytokines. *Blood*. 1997;90(8):3204-3213.

45. Huang W, Yu J, Jones JW, et al. Proteomic Evaluation of the Acute Radiation Syndrome of the Gastrointestinal Tract in a Murine Total-body Irradiation Model. *Health Phys*. 2019;116(4):516-528.

Table 1 Demographics, donor details and transplant conditioning for AHST patients whose biopsies were included in study

Pt UPN	Age (yrs)	Diagnosis	Conditioning	Donor	HLA match
1	32	AML	RIC (Flu/Mel*)	Unrelated	m/m
2	65	CLL	RIC (Flu/Bu)	Unrelated	matched
3	36	CML	RIC (Flu/Mel*)	Related	m/m
4	50	AML	RIC (Flu/Mel*)	Unrelated	m/m
5	51	Myeloma	RIC (Flu/Cy)	Related	matched
6	62	FL (LPD)	RIC (Flu/Cy)	Unrelated	matched
7	62	MDS	RIC (Flu/Cy)	Unrelated	matched
8	47	Myeloma	RIC (Flu/Cy)	Unrelated	matched
9	51	ALL	RIC (Flu/Cy)	Unrelated	matched
10	53	NHL	RIC (Flu/Cy)	Unrelated	matched
11	32	MDS	RIC (Flu/Cy)	Unrelated	matched
12	51	MDS	RIC (Flu/Cy)	Unrelated	matched
13	44	AML	RIC (Flu/Cy)	Related	matched
14	31	ALL	MA (Cy/TBI)	Unrelated	matched
15	62	MDS	RIC (Flu/Cy)	Unrelated	matched
16	58	MCL (LPD)	RIC (Flu/Cy)	Related	matched
17	46	MF	RIC (Flu/Cy)	Related	matched
18	59	CLL (LPD)	RIC (Flu/Bu)	Unrelated	matched
19	41	FL (LPD)	RIC (Flu/Cy)	Unrelated	matched
20	35	CML	MA (Bu/Cy)	Related	matched
21	22	ALL	MA (Bu/Cy)	Unrelated	matched
22	53	AML	RIC (Flu/Cy)	Related	matched
23	57	FL (LPD)	RIC (Flu/Cy)	Unrelated	matched
24	30	ALL	MA (Cy/TBI)	Unrelated	matched
25	63	AML	RIC (Flu/Cy)	Related	matched
26	66	CLL (LPD)	RIC (Flu/Bu)	Unrelated	matched
27	64	MCL (LPD)	RIC (Flu/Cy)	Related	matched
28	42	HD (LPD)	RIC (Beam*)	Unrelated	matched
29	59	AML	RIC (Flu/Cy)	Related	matched
30	51	MDS	RIC (Flu/Cy)	Related	matched
31	43	ALL	RIC (Flu/Cy)	Related	matched
32	41	MDS	RIC (Flu/Cy)	Unrelated	matched
33	33	AA	RIC (Flu/Cy/TBI*)	Unrelated	matched
34	38	ALL	RIC (Flu/Cy)	Related	matched
35	39	CLL (LPD)	RIC (Flu/Mel*)	Unrelated	m/m
36	20	AML	RIC (Flu/Cy)	Unrelated	matched
37	43	MDS	RIC (Flu/Cy)	Unrelated	matched
38	38	ALL	RIC (Flu/Cy)	Unrelated	matched
39	56	MCL (LPD)	RIC (Flu/Cy)	Related	matched
40	53	MDS	RIC (Flu/Cy)	Unrelated	matched
41	41	MCL (LPD)	RIC (Flu/Cy)	Related	matched
42	51	AML	RIC (Flu/Cy)	Related	matched
43	60	CLL (LPD)	RIC (Flu/Bu)	Unrelated	matched
44	64	AML	RIC (Flu/Cy)	Related	matched
45	58	MDS	RIC (Flu/Cy)	Unrelated	matched
46	47	MDS	RIC (Flu/Cy)	Unrelated	matched
47	43	FL (LPD)	RIC (Flu/Cy)	Unrelated	matched
48	65	AML	RIC (Flu/Cy)	Unrelated	matched

49	64	MCL (LPD)	RIC (Flu/Cy)	Related	matched
50	55	CLL (LPD)	RIC (Flu/Bu)	Related	matched
51	48	MDS	RIC (Flu/Cy)	Unrelated	matched
52	57	AML	RIC (Flu/Cy)	Unrelated	matched
53	51	DLBCL (LPD)	RIC (Flu/Cy)	Unrelated	matched
54	52	AML	RIC (Flu/Cy)	Related	matched

AML, acute myeloid leukemia; MDS, myelodysplasia; ALL, Acute lymphoblastic leukemia; MPD, myeloproliferative disorder; CLL, chronic lymphocytic leukemia; FL; Follicular lymphoma; MCL, Mantle cell lymphoma; CML, chronic myeloid leukemia; MF, myelofibrosis; LPD, lymphoproliferative disorder; AA, aplastic anemia; PBSC, peripheral blood stem cells; RIC, reduced intensity conditioning; Flu, Fludarabine; Cy, cyclophosphamide; Bu, Busulphan; Mel, Melphalan; Beam, BCNU, etoposide, Ara-C and Melphalan; MA, myeloablative; TBI, Total body irradiation; matched, HLA-matched (at A, B, C and DR); m/m, HLA mismatched at a single HLA-A or -C locus. * *In vivo* alemtuzumab

Table 2 Effect of clinical variables on GI biopsy sub-crypt RARα^{hi} cell numbers

Variable	Group/number of patients	Sub-crypt RARα^{hi} cell number, mean (+/- SE)	P*
Recipient Age	Below median, n=25	1387 +/- 248	.957
	Above Median, n=25	1407 +/- 280	
Recipient diagnosis	Lymphoid malignancy, n=30	1404 +/- 244	.910
	Myeloid malignancy, n=20	1387 +/- 289	
Donor	Family, n=19	1182 +/- 361	.420
	Unrelated, n=31	1522 +/- 204	
Conditioning	RIC, n=46	1422 +/- 198	.450
	FIC, n=4	1112 +/- 426	
HLA match in GvHD vector	Fully matched, n=46	1231 +/- 169	0.09
	Single antigen mismatch, n=4	3263 +/- 818	
T-cell depletion	No, n=44	1276 +/- 175	.286
	Yes, n=6	2002 +/- 817	
Time to biopsy	Before Day + 180 n=31	1574 +/- 246	.219
	After Day + 180 n=19	1117 +/- 272	
Histological GvHD	No, n=10	498 +/- 85	***<0.001***
	Yes, n=40	1599 +/- 213	

RIC, reduced intensity conditioning; FIC, full intensity conditioning; *unpaired t test without assuming equal variance

Figure 1 RA-responsive mononuclear cells are increased in areas adjacent to GI-GvHD tissue damage

A RARα protein expression measured by flow cytometry in human peripheral blood mononuclear cells (PBMC) allostimulated in the absence or presence of exogenous RA. Example pseudodot plots are shown. Cells with high expression of RARα are shown in Region 1 (R1). **B** RARα protein expression in human PBMC allostimulated in the absence or presence of exogenous RA. Results depict 18 independent experiments. **C** Identification of RARα^{hi} mononuclear cells in GI-biopsies using immunohistochemistry (IHC) staining for RARα (upper panel, brown) with hemotoxylin counterstaining (blue). After antigen retrieval, tissue was stained with rabbit anti-human RARα antibody (Santa Cruz, Clone F-9) for 40 min at RT. Sections were then stained using the Biogenex SuperSensitive™ Polymer-HRP IHC Kit and diaminobenzidine chromogen and counterstained with hematoxylin. Mononuclear cells were identified by size and nuclear staining characteristics (middle panel, blue dots) and RARα staining intensity was digitalized using the Ariol Olympus microscope and automated image analysis system (middle panel, red). A threshold of RARα staining intensity was set to identify cells with high RARα expression (lower panel, yellow dots). RARα^{hi} mononuclear cells (lower panel, black arrows) were distinguished from mononuclear cells with lower expression of RARα (lower panel, green arrows). Scale bar is 10um. **D** Correlation between RARα^{hi} mononuclear cell numbers and cellular RA binding protein (CRABP)I/II^{+} cell numbers in upper and lower GI-biopsies from ASHT patients. Solid and dotted lines denote linear regression and 95% confidence intervals respectively. r and p value is for Pearson correlation. **E** Representative GI-biopsy stained for RARα using conventional IHC and DAB chromogen. Sub-crypt regions are outlined in black and arrowed. Scale bar is 50um. **F** Enrichment of RARα^{hi} mononuclear cell numbers enumerated using the Ariol automated system in sub-crypt regions of GI-biopsies. **G** Representative GI-biopsies stained for RARα using conventional IHC and DAB chromogen from healthy controls and AHST patients with and without histological GvHD. Scale bar is 50um. Black arrows depict mononuclear cells with high

expression of RARα **H** RARα^{hi} mononuclear cell numbers in sub-crypts of GI-biopsies with and without histological GvHD from AHST patients and from healthy controls. **I** Receiver-Operator Curve characteristics for sub-crypt RARα^{hi} cell numbers, RARα^{hi} cell intensity and CRABPI/II^{+} cell numbers and the presence of histological GvHD. **J** RARα^{hi} mononuclear cell numbers in sub-crypts of upper (left) and lower (right) GI-biopsies with and without histological GvHD. Horizontal lines on graphs depict medians. P values are for Mann Whitney tests for panels **B, F,** and ANOVA tests with correction for multiple comparisons for panels **H and J**.

AUC, area under the curve. LR, likelihood ratio. **** p<0.0001 *** p<0.001 ** p<0.01, * p<0.05. ns, not significant.

Figure 2 A targeted candidate protein approach identifies a predicted phenotype of RA-responsive cells in the context of increased microenvironmental IL-23

A Mononuclear cell staining for T-cell lineage markers, transcription factors and the cytokines IL-23 and IL-33 and their receptors using conventional IHC in the same GI biopsy cohort. Scale bar is 100μm. Chromgen is DAB, positive cells are brown. Cells are counterstained with hematoxylin. **B** CD8 and CD4 T-cell numbers enumerated automatically using the Ariol system in sub-crypt regions of upper and lower GI-biopsies from AHST patients with and without histological GvHD. **C** Mononuclear cell numbers enumerated automatically using the Ariol system expressing T-cell transcription factors, cytokines and cytokine receptors in sub-crypt regions of upper and lower GI-biopsies from AHST patients with and without histological GvHD. **D** Volcano plot depicting fold change and statistical significance of RARα^{hi} mononuclear cell numbers and cell numbers expressing T-cell lineage markers, transcription factors, cytokines and cytokine receptors in sub-crypt regions of upper and lower GI-biopsies from AHST patients with and without histological GvHD. **E** Total cellular IL-23 (calculated as the product of the number of IL-23^{+} mononuclear cells and the mean intensity of staining of cells for IL-23) in sub-crypt regions of upper and lower GI-biopsies from AHST patients with and without histological GvHD. **F** Volcano plot depicting correlation co-efficients and statistical significance of numbers of RARα^{hi} mononuclear cells and cells expressing T-cell lineage markers, transcription factors, cytokines and cytokine receptors in sub-crypt regions of upper and lower GI-biopsies from AHST patients. r and p values are for Pearson correlations. Cells expressing CD8, T-bet and IL-23R (circled) were significantly positively correlated with numbers of RARα^{hi} mononuclear cells. Horizontal lines are medians. Other p values are for Mann Whitney tests (**A-E)** **** $p<0.0001$ *** $p<0.001$ ** $p<0.01$, * $p<0.05$. ns, not significant ($p>0.10$)

Figure 3 Sequential immunostaining of GI biopsies

A Representative example of a GI-biopsy stained sequentially for RARα, IL-23R and T-bet using VIP chromogen and hematoxylin counterstain, with positive cells staining purple, and CD8 (using DAB chromogen, staining is brown). Sub-crypt regions are outlined in white. Cells with high and low/no expression of individual markers are indicated with red and black arrows respectively. Scale bar is 25µm. **B** Sequential immunostaining was validated by demonstrating a close correlation between mononuclear cell numbers in sequentially stained sections enumerated using manual counting and mononuclear cell numbers in the same sections stained using conventional single stain IHC and enumerated using automated cell counting with the Ariol system. R and P values are for Pearson correlation co-efficients.

Figure 4 Sequential immunostaining reveals an increase in tissue-specific RARα^{hi} CD8 effector T-cells co-expressing T-bet and IL-23R in GI-GvHD

A-**B** RARα^{hi} CD8 (**A**) and CD4 (**B**) T-cell numbers in sub-crypt regions of upper and lower GI-biopsies from AHST patients with and without histological GvHD and lower GI-biopsies from healthy controls. **C-D** CD8 T-cell numbers co-expressing T-bet (**C**) or IL-23R (**D**) in sub-crypt regions of upper and lower GI-biopsies from AHST patients with and without histological GvHD and lower GI-biopsies from healthy controls. **E** SPICE plots depicting sub-populations of CD8 T-cells in sub-crypt regions of GI-biopsies. Arcs represent median frequencies of CD8 T-cells expressing high RARα, T-bet or IL-23R. Slices represent median frequencies of CD8 T-cell subpopulations by co-expression patterns of RARα, T-bet and IL-23R. Results are shown for upper and lower GI-biopsies from 4 healthy controls and 22 AHST patients, 15 with and 7 without histological GvHD. **F** CD8 T-cell subpopulations expressed as percentage of total CD8 cells in sub-crypt regions of upper and lower GI-biopsies from 4 healthy controls (circles) and 22 AHST patients,15 with (diamonds) and 8 without (triangles) histological GvHD. **G** Absolute numbers of CD8 T-cell subpopulations in sub-crypt regions of GI-biopsies. Color key is as shown in panel **E. H** SPICE plots depicting frequencies of sub-populations of CD8 T-cells in epidermis of skin biopsies from AHST patients. Pie arcs and slices as in **E**. Results are shown for biopsies from 11 AHST patients, 8 with and 3 without histological skin GvHD. **I** Absolute numbers of RARα^{hi} CD4 T-cells co-expressing FOXP3 in sub-crypt regions of GI-biopsies from 12 AHST patients and 4 healthy controls. Numbers of RARα^{hi} T-bet^{+} CD8 effector T-cells in GI-biopsies from AHST patients with histological GvHD are shown for comparison. Horizontal lines and adjacent numbers are medians. P values are for ANOVA with post-test correction for multiple comparisons *** $p<0.001$ ** $p<0.01$, * $p<0.05$. ns, not significant

Figure 5 RARα^{hi} effector T-cells are also selectively expanded in the peripheral blood of GI-GvHD patients

A Representative dot plots and histograms of RARα, IL-23R and T-bet expression on live CD8 T-cells in peripheral blood of an AHST patient at onset of GI-GVHD and an AHST patient without GvHD from a similar time point. CD8 T-cells co-expressing high RARα and IL-23R in boxed region R1 (left) expressed high levels of T-bet (right), whereas RARα$^{dim/neg}$ and IL-23R^{neg} CD8 T-cells in boxed region R2 expressed low levels of T-bet. **B-C** Percentage of live triple positive CD8 (**B**) and CD4 (**C**) T-cells (co-expressing high RARα, T-bet and IL-23R) from peripheral blood from healthy controls (n=4) and ASCT patients with GI- or skin-GvHD (n=7 and 5 respectively) or without GvHD (n=8) at matched time points. **D** Unsupervised phenotypic clustering of live mononuclear cells from samples depicted in **(B)** displayed as Phenograph-generated tSNE plots. Each cluster represents one of 24 phenotypically distinct T-cell subsets. **E** Heat map of relative expression levels of RARα, T-bet, IL-23R and the GI-tropic molecules β_7 and CCR9 of distinct CD3 T-cell clusters displayed in panel **D**. **F-G** Volcano plots depicting fold change and statistical significance of abundance of distinct clusters within the peripheral blood live CD3 T-cell compartment from AHST patients with or without GI-GvHD (**F**) and with GI-or skin-GvHD (**G**). **H** Percentage of live mononuclear cells in cluster 4 in peripheral blood of AHST patients. Horizontal lines are medians. P values are for ANOVA with post-test correction for multiple comparisons (**B**-**C** and **H**) or Mann Whitney tests (**F**-**G**) ** $p<0.01$, * $p<0.05$ trend ($p<0.10$) ns, not significant ($p>0.10$)

Figure 6 The dominant effect of RA on human alloresponses is to increase GI-tropic RARα^{hi} CD8 effector T-cells and is potentiated in IL-23-rich conditions

A Proportion of CD8 and CD4 T-cells proliferating after allostimulation in the absence or presence of RA (0.1 and 1 μM). Results are shown for 9 independent experiments. **B** Heat map of percentage of alloproliferative CD8 and CD4 T-cells expressing GI-tropic molecules, high RARα, the activation marker CD25, the effector T-cell transcription factor T-bet and the CD4 regulatory T-cell transcription factor FOXP3 after allostimulation with/without exogenous RA (1μM). Results depict median values for between 6 and 25 independent experiments. **C** Fold-change in frequency of alloproliferative GI-tropic triple positive (TP) CD8 effector T-cells (co-expressing high RARα, T-bet, IL-23R) after allostimulation with/without exogenous RA (1 μM) and the RARα-specific inhibitor ER-50891 (ER). Results depict 8 independent experiments. **D** Heat map of percentage of alloproliferative CD8 and CD4 T-cells the molecules depicted in (**B)** after allostimulation with exogenous RA (1μM) +/- IL-23. Results depict median values for 12-27 independent experiments except for $\alpha_4\beta_7$ co-expression (3 independent experiments). **E** Percentage of live alloproliferative CD8 T-cells expressing both α_4 and β_7 integrins allostimulated with/without exogenous RA (1μM) +/- IL-23. Results depict 3-9 independent experiments. **F** Ratio of live alloproliferative cells with a CD8 effector T-cell (Teff): CD4 regulatory T-cell (Treg) phenotype after allostimulation with exogenous RA (1μM) +/- IL-23. Results depict 24 independent experiments. **G** Fold-change in frequency of live alloproliferative GI-tropic TP CD8 effector T-cells after allostimulation with/without exogenous RA (1μM) and/or lipopolysaccharide (LPS). Results depict 13 independent experiments. **H** Unsupervised phenotypic clustering of live PBMC after allostimulation with/without exogenous RA (1μM) and LPS displayed as Phenograph-generated tSNE plots. Clusters are derived from 7 independent experiments. **I** Heat map of relative expression levels of RARα, T-bet, IL-23R and the GI-tropic molecules β_7 and CCR9 of distinct cell trace violet (CTV)^{dim} alloproliferative CD3 T-cell clusters. **J** Volcano plot depicting fold change and statistical significance of abundance of distinct T-cell clusters within live PBMC allostimulated with or without RA (1μM)

and LPS. Cluster colors are depicted in panel **I.** **K** Percentage of live mononuclear cells in cluster 7 in PBMC allostimulated in the absence or presence of RA and LPS. **L** Phenotypic heat map for *in vitro* cluster 7 in human PBMC allostimulated with RA and LPS. The phenotype for cluster 4 seen in peripheral blood of GI-GvHD patients is also shown for comparison. CTV, cell trace violet. Horizontal lines are medians. P values are for Wilcoxon matched-pairs signed rank test (**B**, **D, E, J** and **K)** and ANOVA or mixed effects models with post-test correction (**A**, **C**, **E, G)**. **** $p<0.0001$ *** $p<0.001$ ** $p<0.01$, * $p<0.05$. ns, not significant, nd, not done.

Figure 1

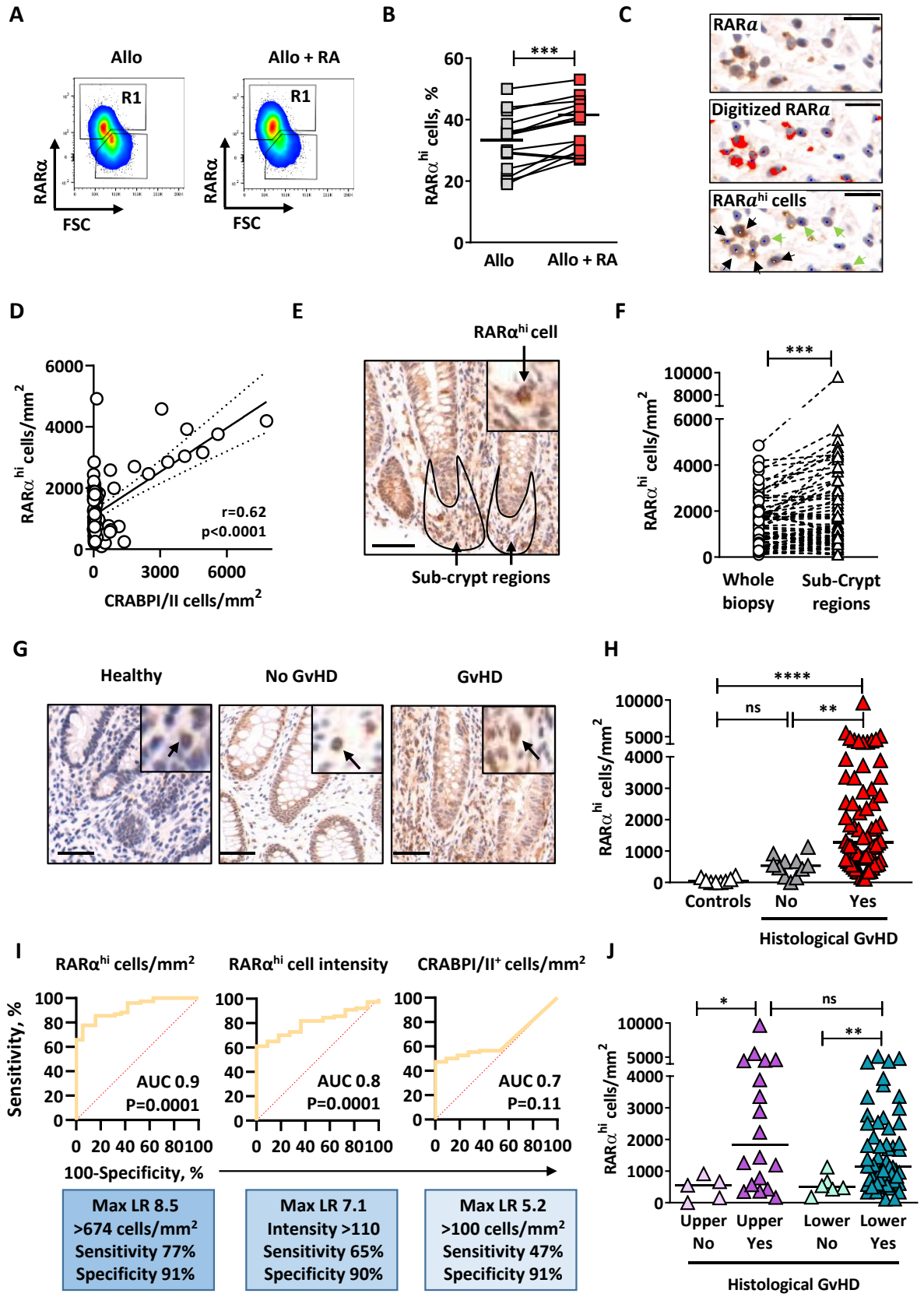
A
Allo
Allo + RA
R1
RARα
FSC
B
***
RARα hi cells, %
Allo
Allo + RA
C
RARα
Digitized RARα
RARα hi cells
D
RARα hi cells/mm2
CRABPI/II cells/mm2
r=0.62
p<0.0001
E
RARα hi cell
Sub-crypt regions
F
RARα hi cells/mm2
Whole biopsy
Sub-Crypt regions
G
Healthy
No GvHD
GvHD
H
****
ns
**
RARα hi cells/mm2
Controls
No
Yes
Histological GvHD
I
RARα hi cells/mm2
RARα hi cell intensity
CRABPI/II+ cells/mm2
Sensitivity, %
AUC 0.9
P=0.0001
AUC 0.8
P=0.0001
AUC 0.7
P=0.11
100-Specificity, %
Max LR 8.5
>674 cells/mm2
Sensitivity 77%
Specificity 91%
Max LR 7.1
Intensity >110
Sensitivity 65%
Specificity 90%
Max LR 5.2
>100 cells/mm2
Sensitivity 47%
Specificity 91%
J
*
ns
**
RARα hi cells/mm2
Upper No
Upper Yes
Lower No
Lower Yes
Histological GvHD

Figure 2

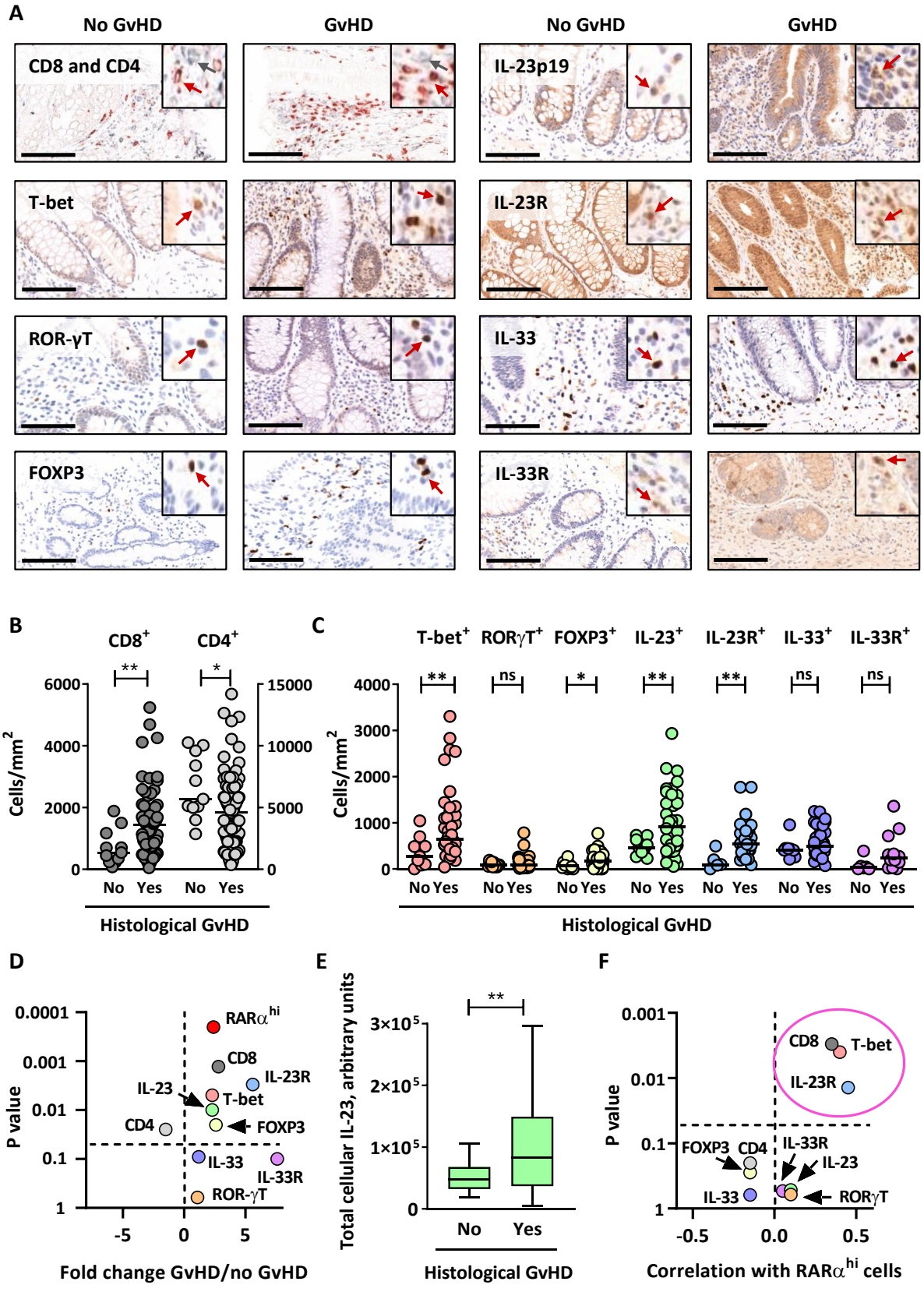
A
No GvHD
GvHD
No GvHD
GvHD
CD8 and CD4
IL-23p19
T-bet
IL-23R
ROR-γT
IL-33
FOXP3
IL-33R
B
CD8+
CD4+
Cells/mm2
Histological GvHD
C
T-bet+
RORγT+
FOXP3+
IL-23+
IL-23R+
IL-33+
IL-33R+
Cells/mm2
Histological GvHD
D
P value
Fold change GvHD/no GvHD
RARα hi
CD8
IL-23R
IL-23
T-bet
CD4
FOXP3
IL-33
IL-33R
ROR-γT
E
Total cellular IL-23, arbitrary units
Histological GvHD
F
P value
Correlation with RARα hi cells
CD8
T-bet
IL-23R
FOXP3
CD4
IL-33R
IL-23
IL-33
RORγT

Figure 3

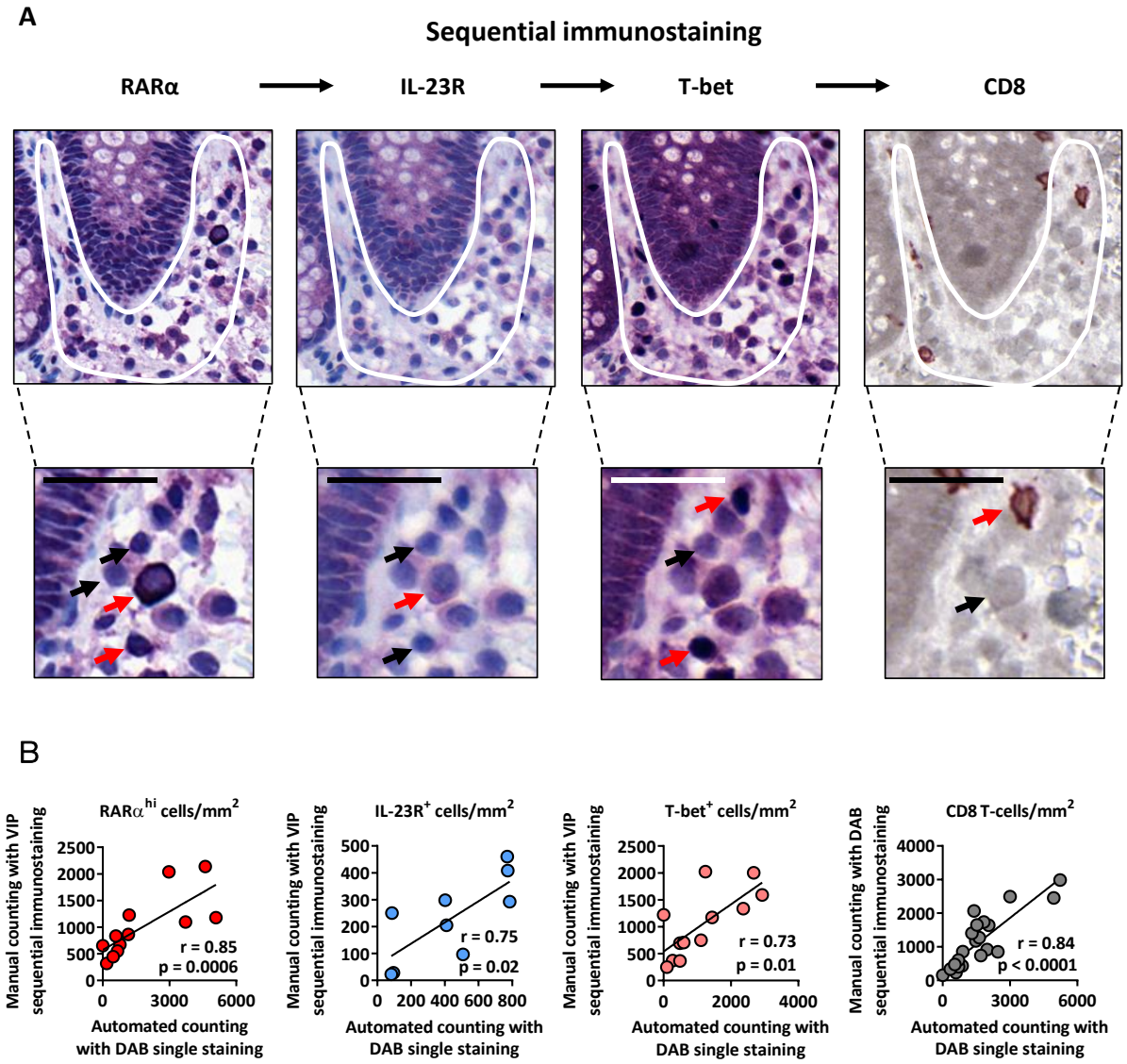
A
Sequential immunostaining
RARα
IL-23R
T-bet
CD8
B
RARα hi cells/mm2
Manual counting with VIP sequential immunostaining
Automated counting with DAB single staining
r = 0.85
p = 0.0006
IL-23R+ cells/mm2
r = 0.75
p = 0.02
T-bet+ cells/mm2
r = 0.73
p = 0.01
CD8 T-cells/mm2
Manual counting with DAB sequential immunostaining
r = 0.84
p < 0.0001

Figure 4

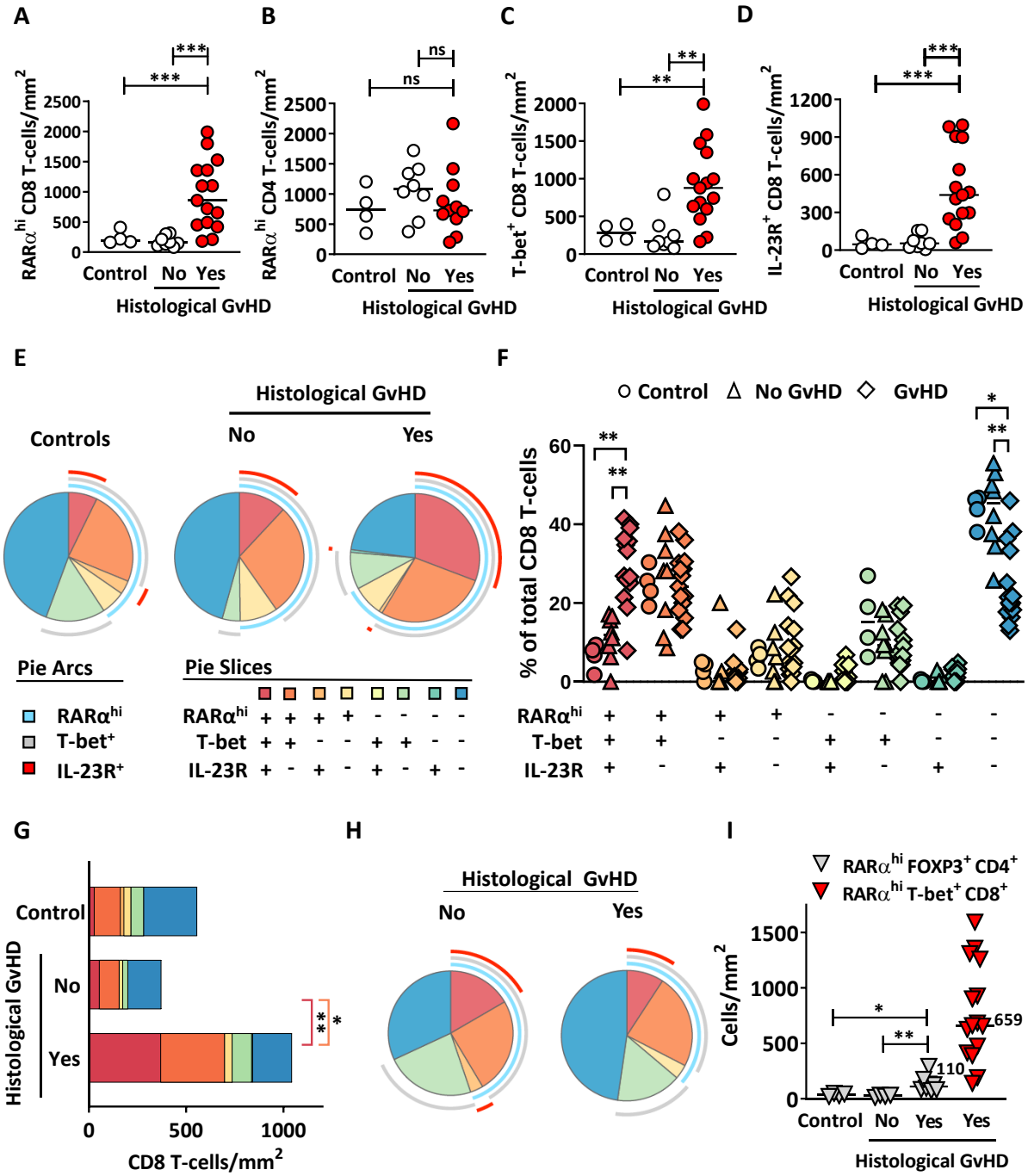
A
B
C
D
RARα^hi CD8 T-cells/mm^2
RARα^hi CD4 T-cells/mm^2
T-bet^+ CD8 T-cells/mm^2
IL-23R^+ CD8 T-cells/mm^2
Control No Yes
Histological GvHD
ns
E
Controls
Histological GvHD
No
Yes
Pie Arcs
RARα^hi
T-bet^+
IL-23R^+
Pie Slices
F
Control
No GvHD
GvHD
% of total CD8 T-cells
G
Control
No
Yes
Histological GvHD
CD8 T-cells/mm^2
H
I
RARα^hi FOXP3^+ CD4^+
RARα^hi T-bet^+ CD8^+
Cells/mm^2
659
110

Figure 5

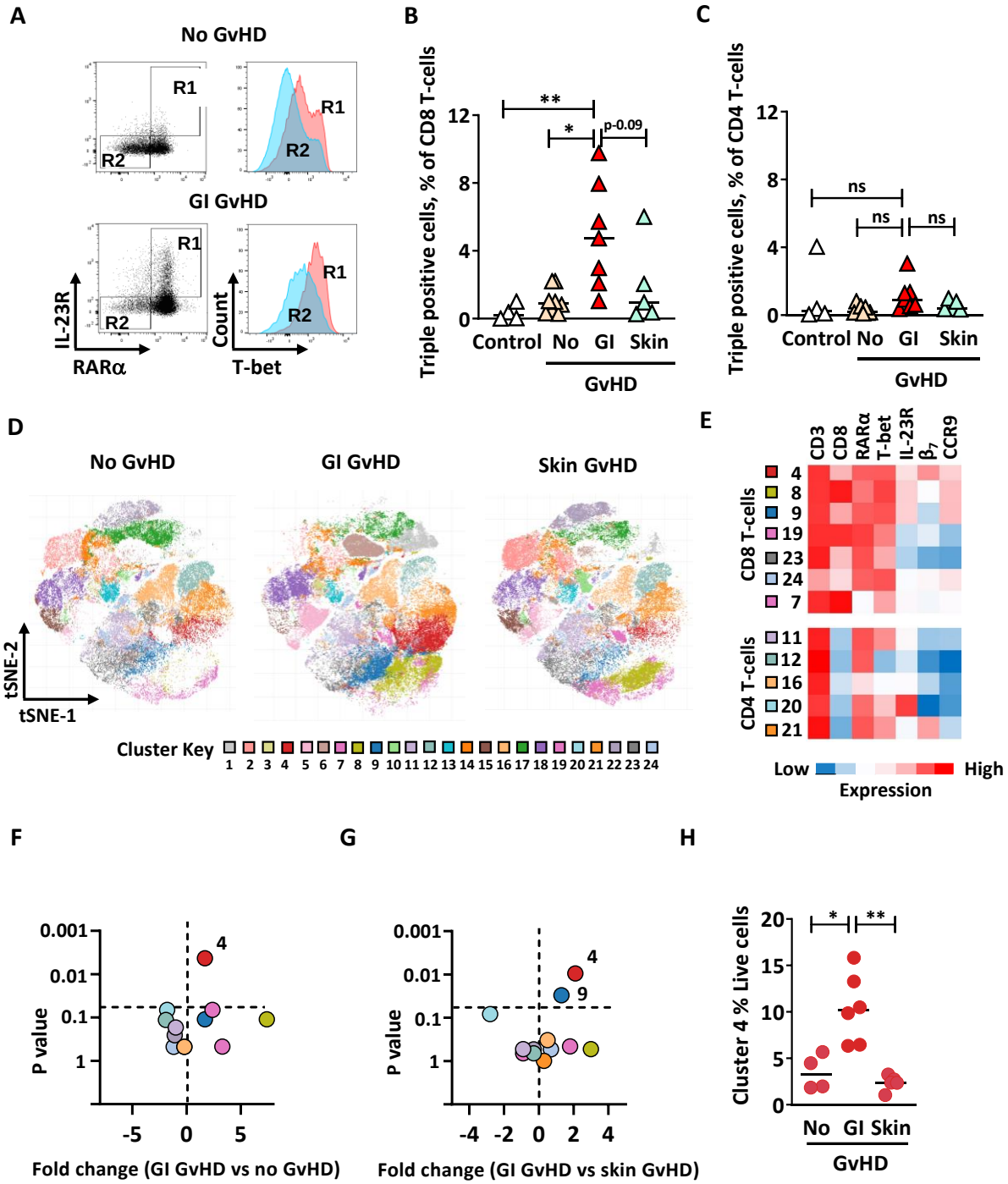
A
No GvHD
R1
R2
GI GvHD
IL-23R
RARα
Count
T-bet
B
Triple positive cells, % of CD8 T-cells
Control
No GvHD
GI GvHD
Skin GvHD
p-0.09
C
Triple positive cells, % of CD4 T-cells
ns
D
No GvHD
GI GvHD
Skin GvHD
tSNE-2
tSNE-1
Cluster Key
E
CD3
CD8
RARα
T-bet
IL-23R
β7
CCR9
CD8 T-cells
CD4 T-cells
Low
High
Expression
F
P value
Fold change (GI GvHD vs no GvHD)
G
Fold change (GI GvHD vs skin GvHD)
H
Cluster 4 % Live cells

Figure 6

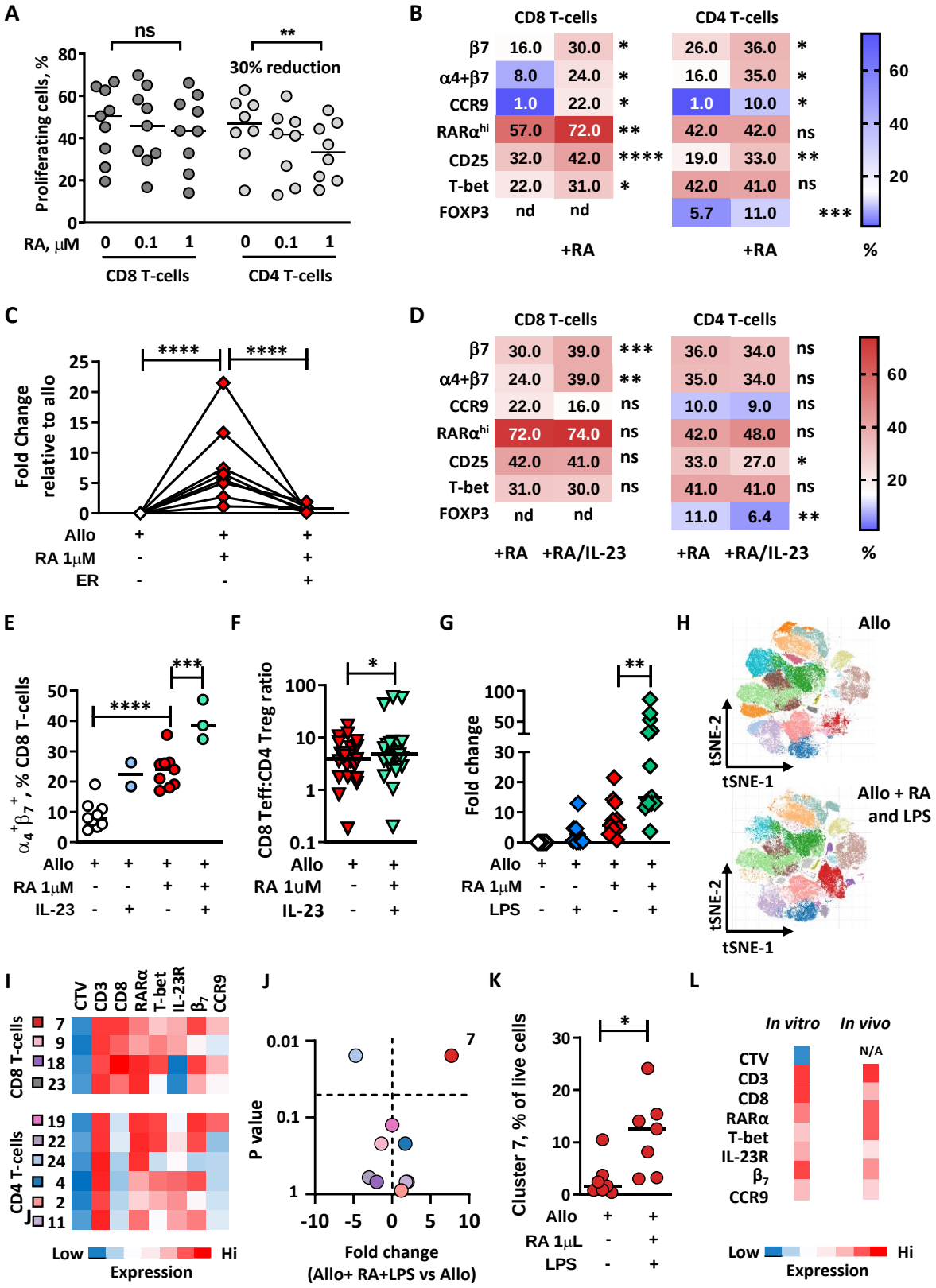
A
ns
**
30% reduction
Proliferating cells, %
RA, μM 0 0.1 1 0 0.1 1
CD8 T-cells
CD4 T-cells
B
CD8 T-cells
CD4 T-cells
β7 16.0 30.0 * 26.0 36.0 *
α4+β7 8.0 24.0 * 16.0 35.0 *
CCR9 1.0 22.0 * 1.0 10.0 *
RARα^hi 57.0 72.0 ** 42.0 42.0 ns
CD25 32.0 42.0 **** 19.0 33.0 **
T-bet 22.0 31.0 * 42.0 41.0 ns
FOXP3 nd nd 5.7 11.0 ***
+RA +RA %
C
****
****
Fold Change relative to allo
Allo + + +
RA 1μM - + +
ER - - +
D
CD8 T-cells
CD4 T-cells
β7 30.0 39.0 *** 36.0 34.0 ns
α4+β7 24.0 39.0 ** 35.0 34.0 ns
CCR9 22.0 16.0 ns 10.0 9.0 ns
RARα^hi 72.0 74.0 ns 42.0 48.0 ns
CD25 42.0 41.0 ns 33.0 27.0 *
T-bet 31.0 30.0 ns 41.0 41.0 ns
FOXP3 nd nd 11.0 6.4 **
+RA +RA/IL-23 +RA +RA/IL-23 %
E
***
****
α4+β7+ % CD8 T-cells
Allo + + + +
RA 1μM - - + +
IL-23 - + - +
F
*
CD8 Teff:CD4 Treg ratio
Allo + +
RA 1uM - +
IL-23 - +
G
**
Fold change
Allo + + + +
RA 1μM - - + +
LPS - + - +
H
Allo
tSNE-2
tSNE-1
Allo + RA and LPS
tSNE-2
tSNE-1
I
CTV CD3 CD8 RARα T-bet IL-23R β7 CCR9
CD8 T-cells 7 9 18 23
CD4 T-cells 19 22 24 4 2 11
Low Hi
Expression
J
P value
7
Fold change (Allo+ RA+LPS vs Allo)
K
*
Cluster 7, % of live cells
Allo + +
RA 1μL - +
LPS - +
L
In vitro
In vivo
N/A
CTV
CD3
CD8
RARα
T-bet
IL-23R
β7
CCR9
Low Hi
Expression